ISSN 1069-3513, Izvestiya, Physics of the Solid Earth, 2008, Vol. 44, No. 10, pp. 846–855. © Pleiades Publishing, Ltd., 2008.
Original Russian Text © V.A. Petrov, Niu Anfu, V.B. Smirnov, A.O. Mostryukov, Li Zhixiong, A.V. Ponomarev, Jiang Zaisen, Shen Xuhui, 2008, published in Fizika Zemli, 2008, No. 10, pp. 101–112.

Field of Tectonic Stresses from Focal Mechanisms of Earthquakes and Recent Crustal Movements from GPS Measurements in China

V. A. Petrov[a], Niu Anfu[d], V. B. Smirnov[b, c], A. O. Mostryukov[a], Li Zhixiong[d], A. V. Ponomarev[b], Jiang Zaisen[d], and Shen Xuhui[d]

[a] Borok Geophysical Observatory (BGO), Schmidt Institute of Physics of the Earth, Russian Academy of Sciences (RAS), Borok, Yaroslavl oblast, 119991 Russia

[b] Schmidt Institute of Physics of the Earth, RAS, Bol'shaya Gruzinskaya ul. 10, Moscow, 123995 Russia

[c] Department of Physics, Moscow State University, Moscow, 117234 Russia

[d] Institute of Earthquake Sciences, Chinese Academy of Sciences, Beijing, 100080 China

Received May 14, 2008

Abstract—Orientations of the principal axes of the tectonic stress field reconstructed from seismological data on focal mechanisms of earthquakes and strain fields determined from GPS measurements in China are compared. The data of GPS measurements used in the paper were obtained by the Crustal Movement Observation Network of China (about 1000 stations) in the period of 1998–2004. On the basis of information on the recent horizontal crustal motions, the strain field is calculated for the study territory by the finite element method. Calculations of the strain tensor using GPS data were carried out with a step of 1° in latitude and longitude. A catalog of earthquake focal mechanisms was used for the reconstruction of tectonic stress field components. Focal mechanisms of earthquakes were calculated with the use of seismological data on signs of first arrivals from the bulletin of the International Seismological Center. To estimate characteristics of the regional stress field, an approach based on the kinematic method proposed by O.I. Gushchenko was applied. The tectonic stress field was reconstructed in depth intervals of $0 < H < 35$ km and 35 km $< H < 70$ km from data on focal mechanisms of earthquakes over the periods of 1998–2004 and 1985–2004. Comparison of directions of the principal strain axes at the surface (according to GPS measurements) and directions of the principal stress axes (reconstructed from focal mechanisms of earthquakes) showed their good convergence. Seismotectonic strains and GPS measurements coincide within a larger part of the territory. The coincidence is best in a depth interval of $0 < H <$ 35 km. Maximum misfit values are confined to areas of high 3-D gradients of strain axis directions and are possibly related to the structural heterogeneity of the region, zones with strains of the same type along both horizontal axes (compression or extension along all directions), or areas of small absolute values of recent horizontal movements. Areas with invariable directions of the stress axes are recognizable regardless of the depth of initial data. Good reproducibility of results obtained by two different methods made it possible to check the method of stress field reconstruction using data on focal mechanisms of earthquakes.

PACS numbers: 91.30.Dk

DOI: 10.1134/S1069351308100121

INTRODUCTION

The modern level of research on deformation processes in the Earth's crust and lithosphere is inaccessible without information on tectonic stresses in these regions. The stress–strain states of the crust and upper mantle are the most important factors, determining the nature of tectonic processes and development of related tectonic movements, strains, folds, and faults.

In this context, the development of methods and approaches for the reconstruction of tectonic stress fields is a significant task of tectonophysics, geotectonics, and seismology. The fulfillment of this task is of great importance for a number of theoretical and applied problems of geophysics, geology, and mining engineering and is closely related to earthquake prediction; the interpretation of recent movements; assessement of the seismic hazard; and research on physics of phenomena observed in a source region before, during, and after an earthquake.

At the present time, a whole series of methods has been developed for the reconstruction of stress and strain tensors on the basis of various physical principles and various data. Comprehensive reviews and analysis of methods used for the reconstruction of tectonic stresses can be found in [Mukhamediev, 1993; Mukhamediev et al., 2005; Rebetsky, 1999, 2002, 2007]. Information obtained by these methods is undoubtedly of great significance for the solution of various theoretical and applied problems of geophysics, geology, and mining engineering. However, discus-

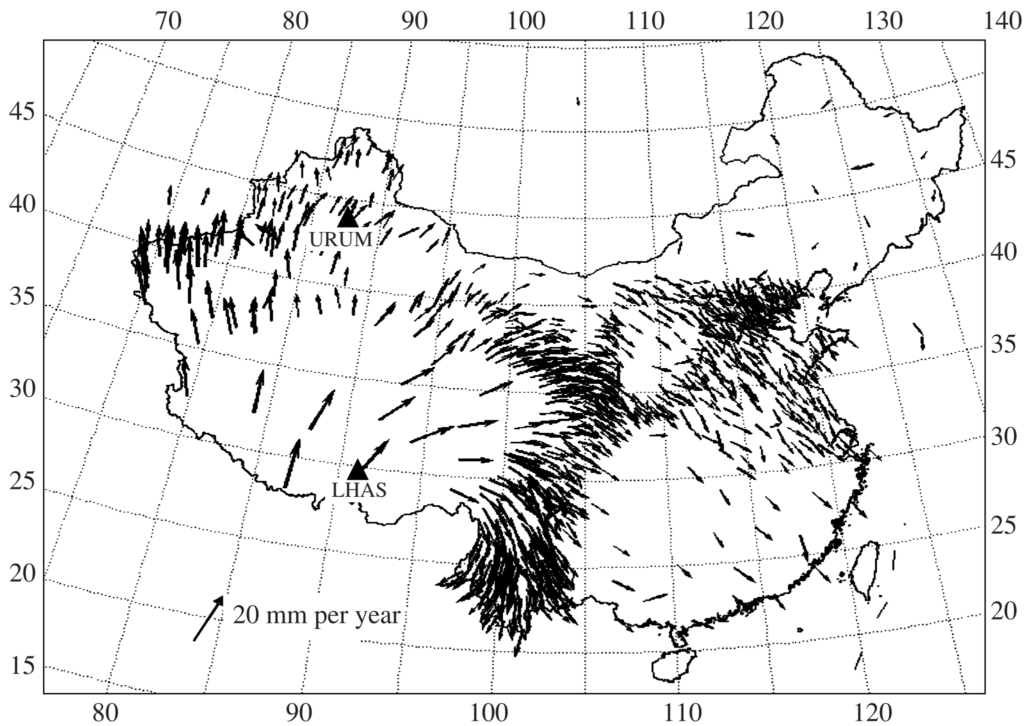

Fig. 1. Distribution of the displacement velocities from GPS data on the territory of China.

sions and disputes concerning the advantages and disadvantages of the methods are continuing. Verification of the methods even between themselves has not been carried out. To check the correctness of regional reconstructions of stress and strain fields obtained by different methods from geological or seismological data, methods providing instrumental information for large regions did not exist until recently.

The strain pattern of the crust attracts much interest and is widely discussed in modern geotectonics. Identification of blocks in the spatial field of the velocity of horizontal movements for solution of geodynamic problems was studied [Gatinskii et al., 2005; Zubovich et al., 2004; Mukhamediev et al., 2006; Parsons, 2006]. Recently, data of GPS measurements and other positioning systems are being more actively invoked for solving geodynamic problems. On the basis of these data, new global models of motion of lithospheric plates were developed and regional characteristics of contemporary crustal strains were studied in detail. In our opinion, the meaningful result of these studies is in many cases the inconsistency and misfit of GPS measurements with geological reconstructions and seismological data. The value and origin of this misfit are not quite clear.

The present work compares results of reconstruction of the tectonic stress field from data on focal mechanisms of earthquakes with GPS measurements of recent horizontal displacements of the Earth's surface. This comparison was conducted in order to elucidate how adequately surface data of GPS measurements reflect deformations in the lithosphere and to verify the method of stress field reconstruction from data on focal mechanisms of earthquakes.

DATA ON RECENT HORIZONTAL CRUSTAL MOVEMENTS IN CHINA

We used data on recent horizontal crustal motions obtained at the Crustal Movement Observation Network of China. This network contains about 1000 stations. Continuous measurements are made at 25, while the sampling frequency of recording is 1 yr at 56 stations and 2 yr at the remaining stations. If necessary, some stations can operate in a continuous recording regime. The position of the network stations on the territory of China and the distribution of the displacement velocities for these stations are shown in Fig. 1. As seen from Fig. 1, the spatial distribution of stations is very irregular, the majority of the stations being located in eastern China. At present, the western part of the observation system is represented by a sparse network of stations, primarily due to the inaccessibility of territories and their weak population density.

In China, technologies of satellite geodesy used for the determination of velocities of recent crustal movements started to be intensely developed from 1998. These observations provided important information on the movement and deformation patterns of the Earth's surface. The information on the velocities of recent

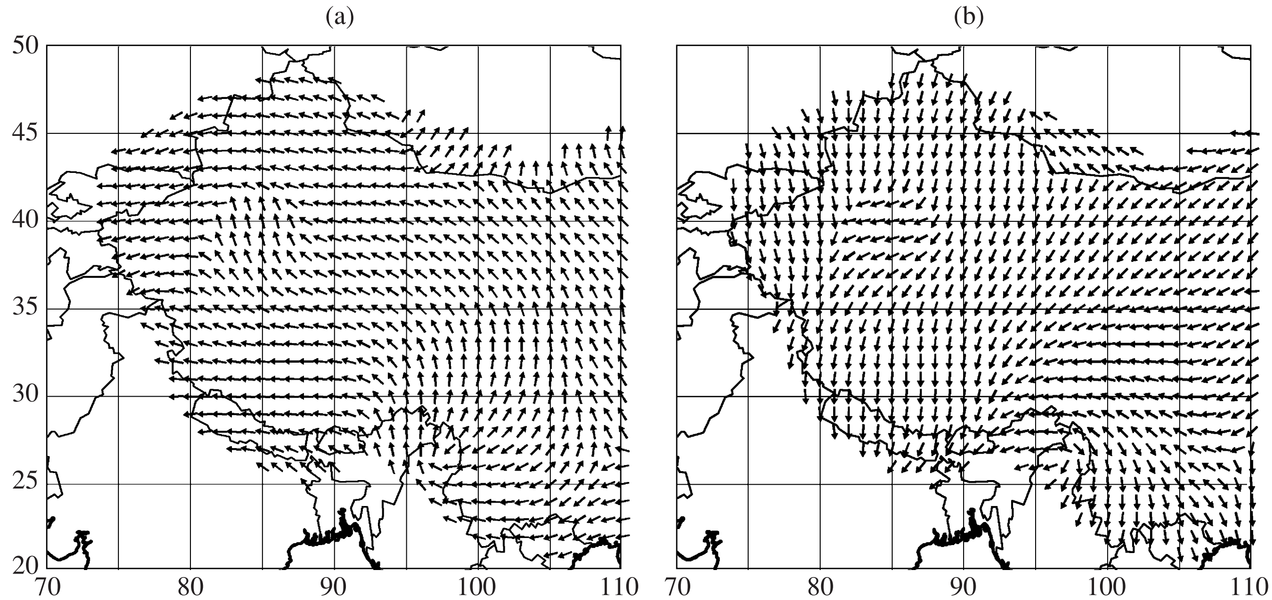

Fig. 2. Spatial distribution of the strain (extension and compression) axes modeled with regard for the strain rate values ($\times 10^{-9}$ 1/yr) from GPS data: (a) orientation of relative extension axes; (b) orientation of relative compression axes.

crustal movements in China and results of its processing were reflected in numerous publications. In this paper, without going into detail of the data processing, it is necessary to note the main achievements of the study of the strain state in the junction zone of the Indian and Asian plates. GPS measurements and their analysis and generalization revealed specific features of recent movements and provided constraints on the deformation of both the Asian region as a whole [Gatinskii et al., 2005; Larson et al., 1999] and its separate areas [Zubovich et al., 2004; Mukhamediev et al., 2006; Chen et al., 2000]; the spatial distribution of strains over the territory of China was also obtained [Ma et al., 2001; Liang et al., 2003a, 2003b; Ying et al., 1999]. The study of crustal movements from GPS measurements provided insights into the relation between regional deformation and seismicity. These results were successfully used for prediction of the earthquake of November 14, 2001, with the magnitude $M = 8.1$ [Liang et al., 2003a, 2003b; Gu et al., 2004].

In the present work, we used results of calculation of the strain rate tensor from GPS data obtained in [Liang et al., 2003b] for the territory of China. The velocity of horizontal crustal movements was estimated by the finite element method using real GPS measurements and data on the tectonic structure of China. The strain rate tensor was calculated with a step of 1° in latitude and longitude from data recorded in 1998–2004 (Fig. 2). Figure 2 shows the spatial orientation of axes of relative extension (Fig. 2a) and relative compression (Fig. 2b). Liang et al. [2003b] note that the obtained results revealed main tendencies of crustal movements in the territory of China. However, the information on the strain field obtained for the territory of China requires further refinement because of the inadequate accuracy of the obtained modeling results primarily caused by the nonuniform distribution of stations and the need for further improvement of the modeling technique with the use of additional data.

METHOD OF RECONSTRUCTION OF THE TECTONIC STRESS FIELD

The tectonic stress field was reconstructed by the kinematic method proposed by Gushchenko [1979b]. The method was realized as an algorithm of description of space–time variations in characteristics of a regional stress field taking into account the initial accuracy and different determinations of focal mechanisms of earthquakes [Gushchenko et al., 1990]. A method of retrieval of information on the directions of principal stress axes from a set of focal mechanisms of earthquakes is described in [Gushchenko, 1979a, 1979b, 1982; Petrov et al., 1994, 2002].

In view of the goals of our paper, we thought it appropriate to describe here the method of reconstructing the tectonic stress field from the seismological information on focal mechanisms of earthquakes. In doing so, we tried to emphasize its main features that influence, in our opinion, the determination accuracy of directions of the principal stress axes (σ_1, σ_2, σ_3). The understanding and consideration of these features will possibly be helpful for comparing the obtained directions of the stress tensor axes with the axes of the strain rate tensor determined from GPS data in order to elucidate the origin of their discrepancy.

For the spatial reconstruction of the principal stress axes, the region under study is divided by a uniform grid. The grid spacing depends, first of all, on the problem to be solved and the amount of initial information on focal mechanisms of earthquakes. In the neighborhood of each node of the grid, circular horizontal samples (elementary cells) are formed from a general catalog for a given radius and an initial (minimal) number of focal mechanisms required for the localization of the range of directions admissible for the orientation of the axes σ_1 and σ_3. In our study, this minimal set contains no less than 20 focal mechanisms of earthquakes. Samples of a given radius that do not contain the minimal number of focal mechanisms are not included in calculations. Within the elementary sample, the selected earthquakes are distributed according to the degree of proximity of earthquake coordinates to coordinates of a node. In what follows, the distance between focal mechanisms of earthquakes and nodes determines the order of their summation.

Before considering the method of determination of regional stress field characteristics, we define the terms used for its description. We remind the reader that, in seismology, the directivity diagram of a *P* wave shear source is characterized by a distribution of compression and dilation regions over quadrants. Two nodal planes, which separate alternating quadrants and characterize the slip in an earthquake source, define two mutually orthogonal equiprobable directions. In a focal mechanism, two crosswise lying quadrants of a spherical space within which negative signs of first displacements in *P* waves are recorded (dilation quadrants) are regions of this space forbidden for the σ_1 axis direction, while the other two quadrants with positive signs of *P* wave first arrivals (compression quadrants) are forbidden for the σ_3 axis direction. Then, one should expect that two mutually orthogonal directions with stable orientation belong to volumes uniform for the entire set of focal mechanisms. One of these directions is not overlapped in stereograms by quadrants of dilation corresponding to these mechanisms, whereas the other direction is not overlapped by quadrants of compression for the entire set of focal mechanisms. The first of these directions should coincide with the direction of the σ_1 axis, while the second should coincide with the direction of the σ_3 axis. Consequently, in order to determine the directions of these axes, it is sufficient to calculate two stereograms, one of which summarizes the entire set of spherical areas overlapped by quadrants of dilation (forbidden for the σ_1 axis direction) and another one summarizes quadrants of compression (forbidden for the σ_3 axis). Identification of stereogram regions that are not overlapped by corresponding quadrants allows one to localize regions admissible for directions of the principal stress axes. In order to determine these directions, it is necessary to take into account the determination accuracy of focal mechanisms of earthquakes and their different determinations for a given earthquake (diversity of the initial data). These general prerequisites were incorporated by Gushchenko into the kinematic method of reconstruction of stresses. Below, we consider in grater detail the algorithm of determination of the orientation of principal stress axes in the elementary volume.

The region of admissible orientations of the principal axes of extension and compression (designated here as σ_1 and σ_3, respectively) is determined by consecutive separate summation (superposition) of quadrant areas of compression and extension in the stereographic projection of the lower hemisphere, taking into account the accuracy and diversity of the initial data [Gushchenko, 1979a, 1981, 1982]. This region is localized as a region of minimum density values of dilation quadrants for the σ_3 axis and compression quadrants for the σ_1 axis. The localization of regions of principal axes is carried out for the chosen sampling frequency along the entire surface of a hemisphere with a *step of about 6°*. The directions of the principal stress axes are calculated as the geometric centers of bundles of directions that contain variants of mutually orthogonal orientations of the σ_1 and σ_3 axes if such variants exist. In this case, the focal mechanisms of earthquakes are considered to be consistent over the entire sample, and the stress field in the volume under study is considered to be homogeneous with respect to the orientation of principal axes.

The summation of forbidden zones in the algorithm is carried out without a validity check as long as regions with zero values of density remain in one or two composite diagrams. Zero density values in the diagrams can also remain up to the end of summation if, at a given sample radius, a limited amount of focal mechanisms is located near a node or all mechanisms in the sample are mutually consistent. In this case, upon attaining the given value of the sample radius, mutually orthogonal variants are found in the regions of solution and the directions of the principal stress axes are calculated. After this, the calculations are terminated. If the amount of data in a sample is sufficient, the summation continues until the region with zero density values disappears in one or (simultaneously) two diagrams. This takes place in the case of the presence of at least one mechanism (below, we call them inconsistent) that is at variance with any direction of one or two axes due to the possible uncertainty of its determination and the imperfections of the faulting model involved in the determination of focal mechanisms. After such a mechanism is encountered, each step of summation is analyzed: the sizes of minimum density areas are checked in each of the diagrams and the presence of mutually orthogonal variants of axis directions is also checked. If mutually orthogonal variants of orientation exist and the sizes of minimum density areas are greater than given values (*in our algorithm their sizes are limited by 20°*), the summation continues. If mutually orthogonal variants of orientation are absent in the solution regions with a minimum density, the given inconsistent mechanism is rejected and calculations are terminated at the preceding step. A similar technique is applied if there are no orthogonal variants of orientation immediately after the inclusion of the first inconsistent mechanism into the sample. In both cases, if the deviation from the orthogonality of the directions σ_1 and σ_3 is greater than 6°, the sample of earthquake sources is considered to be inconsistent and the stress field of the given volume is regarded to be inhomogeneous in space and possibly in time. The value of deviation from orthogonality is considered as a measure of the focal mechanism misfit (or a noise level) in the given sample.

The summation can lead to a situation when the size of the area is less than 20° for one axis and is more than 20° for the other (a possible indication for a deformation mechanism close to uniaxial compression or extension). We consider this case as intermediate and, after the output of the obtained directions σ_1 and σ_3, the summation is continued. The accomplishment of calculations with areas of small sizes characterized by a minimum density and the presence of mutually orthogonal pairs of solutions in two diagrams is considered as an indication that the orientations of the principal stress axes σ_1 and σ_3 are determined reliably and are mutually consistent.

After the accomplishment of calculations, the initial information on focal mechanisms of earthquakes used for the determination of principal stress axis directions is analyzed. A new sample radius (characterizing the size of an elementary homogeneous volume), the number of mechanisms in the sample, and the coordinates of the geometric center of these data are calculated for this set of focal mechanisms. With these new coordinates, the obtained directions of the principal stress axes are recorded into the database.

As noted above, this is an algorithm for the determination of directions of the principal stresses σ_1 and σ_3 in an elementary cell (a sample). Analogous calculations are performed at all grid nodes (satisfying the initial parameters) for the region studied. Finally, after the accomplishment of calculations at all nodes, we have a discrete set of points with known directions of the principal stress axes in the region studied. Since the coordinates of the geometric center of a sample generally do not coincide with the coordinates of the initial grid node, the results should have been reduced to a unified form for the comparison of the axis directions with the strain rate tensor (these calculations were carried out with a step of 1° in latitude and longitude). This problem was solved by interpolation of the field of seismotectonic stress directions on the corresponding grid. Passing to a grid with a spacing of 1°, the total stress tensor was calculated at each node using points nearest to it, and the directions of the largest relative compression and extension in the horizontal plane (below, called horizontal compression and extension) were determined from this tensor.

RESULTS AND DISCUSSION

In the present work, we used a catalog of focal mechanisms of earthquake sources over the period from 1964 through 2005 obtained by processing of data on signs of first arrivals from the bulletin of the International Seismological Center (http://www.isc.ac.uk). Fault plane solutions were obtained using the methodological approaches proposed in [Mostryukov and Petrov, 1994].

We should note that the stress field reconstruction for China was already performed previously, and the main results of these studies were presented in [Gushchenko, 1979b; Petrov et al., 1994, 2002; Rebetsky et al., 1997].

As mentioned above, we used results of calculation of the strain rate tensor from GPS data obtained in [Liang et al., 2003a] for the territory of China. The calculations of the strain rate tensor from GPS data were originally carried out for the entire territory of China. However, the spatial analysis of available data on focal mechanisms of earthquakes and, particularly, the subsequent reconstructions of the stress field from these data showed that the seismological information is insufficient for the eastern part of the territory studied. For this reason, all results of the reconstruction of the tectonic stress field and all further comparisons of them with GPS data are presented for seismically active regions of China and adjacent territories in the area (20°–50°N, 70°–105°E) (the inset in Fig. 3). Considering that the axes of relative lengthening and shortening of the strain rate tensor obtained from GPS data are orthogonal, as well as the horizontal axes of the stresses calculated from focal mechanisms, only the axes of relative lengthening are shown in all subsequent figures and all comparisons are carried out for their directions.

At the first stage of the study, the tectonic stress field was reconstructed for the time interval of initial GPS data from 1998 through 2004 for a depth interval of $0 < H < 35$ km. Figure 3 illustrates results of this reconstruction. As seen from the figure, the seismological information on focal mechanisms for this time interval was insufficient for gaining information required for the comparison with the axes of the strain rate tensor.

Therefore, at the second stage, the tectonic stress field of China was reconstructed from focal mechanisms of earthquakes over the period of 1985–2004 in a depth interval of $0 < H < 35$ km. The spatial distribution of the horizontal extension axes of seismotectonic stresses within this period is presented in Fig. 4, showing that the amount of the obtained information became sufficient for comparison. However, a question arises concerning the validity of the change in the time interval and its influence on the results of reconstruction. In other words, to what extent does the stress field remain stationary with a change in the calculation interval and is it possible to use results obtained in a different time interval for comparison with the axes of the strain rate

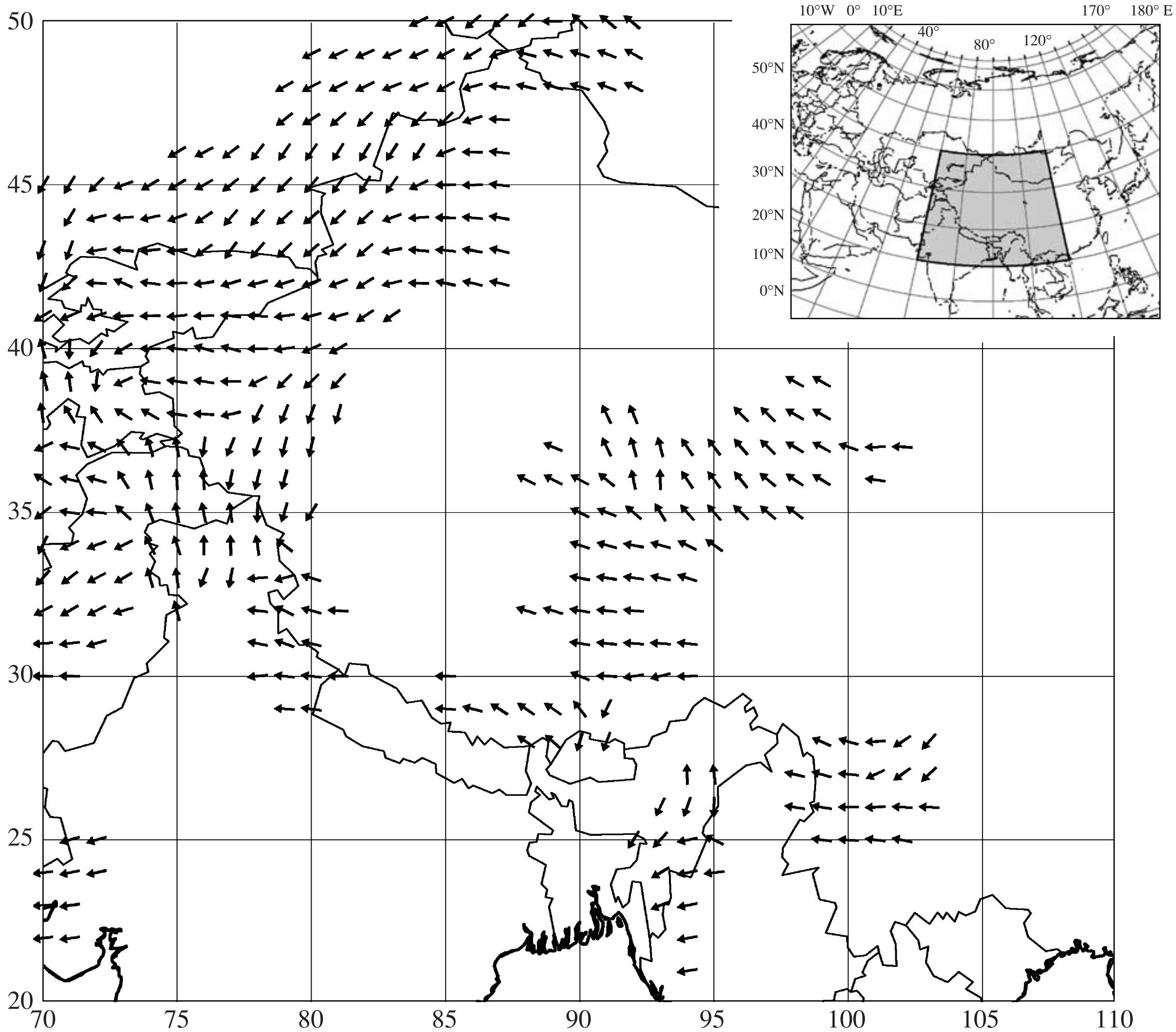

Fig. 3. Spatial distribution of tensile stress tensor axes in the territory of China from focal mechanisms of earthquakes over the time period 1998–2004 in a depth interval of $0 < H < 35$ km. The position of the region under study is shown in the inset.

tensor? To answer this question, results of reconstructions of the tectonic stress field obtained for different calculation intervals were compared.

The spatial distribution of extension axes over 1998–2004 is presented in Fig. 5, where isolines show the value of the azimuth misfit (in degrees) of the horizontal seismotectonic tensile strains over time intervals of 1998–2004 and 1985–2004 in a depth interval of $0 < H < 35$ km. The histogram of the azimuth misfit (in degrees) between the directions of the maximum extension axes obtained over different periods is shown in the inset in Fig. 5. Analogous histograms are shown in the subsequent figures. The comparison of the extension axis directions for two time intervals showed their good convergence, which is confirmed by the distribution of their misfits. Results of the comparison imply that the stress field (the field of the axis directions) remains stationary with the lengthening of the time interval. The misfits are largest in areas characterized by high spatial gradients of the stress ellipsoid axis directions or at the boundary of the region under study where the initial data do not always encircle a node center. This conclusion validates all subsequent reconstructions of the stress field and the comparison of their resulting strain rate tensor axes for a time interval of 1985–2004, although this should be done very cautiously.

The spatial distribution of extension axes over a time interval of 1985–2004 is presented in Fig. 6, where isolines show the azimuth misfit between the seismotectonic tensile strain axes over 1985–2004 and the axes of the tensile strain rate tensor calculated from GPS data (over a time interval of 1998–2004) for a depth interval of $0 < H < 35$ km. The seismotectonic strains and GPS measurements coincide for the larger part of the territory. This suggests that plastic strains in the near-surface part of the crust that are not accounted for by the seismotectonic strain are either small or have

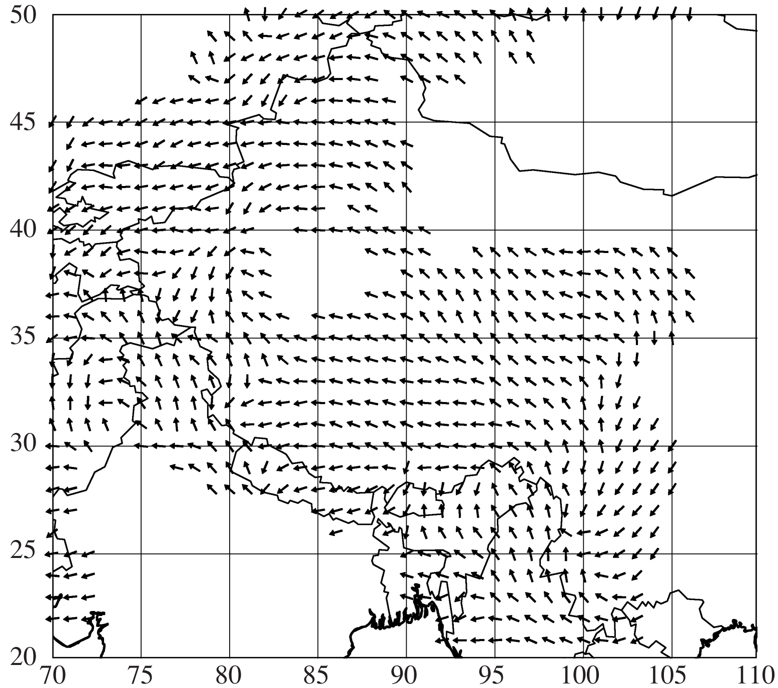

Fig. 4. Spatial distribution of tensile stress tensor axes in the territory of China from the focal mechanisms of earthquakes over the period 1985–2004 in a depth interval of $0 < H < 35$ km.

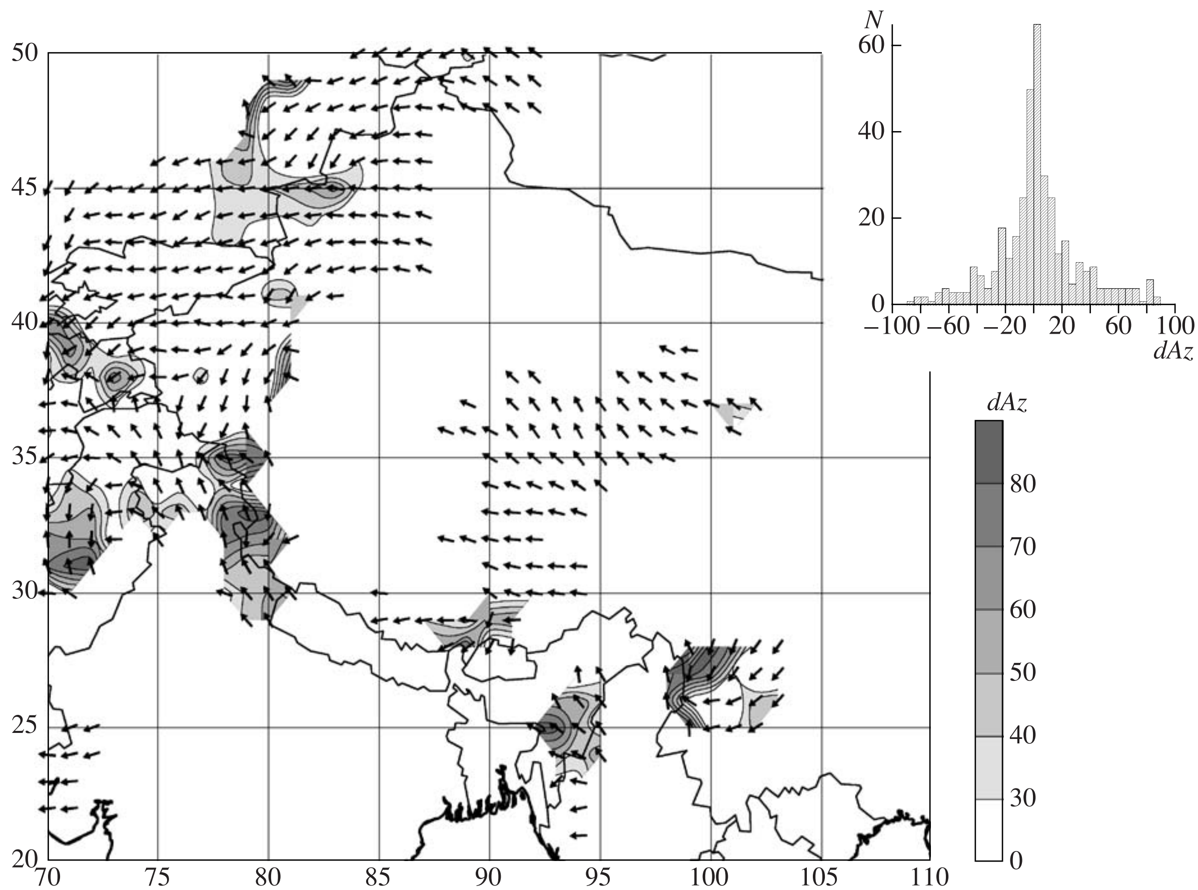

Fig. 5. Azimuth misfits of horizontal seismotectonic strain directions over the periods 1998–2004 and 1985–2004 in a depth interval of $0 < H < 35$ km (the orientations of extension axes over the same period are shown by arrows). Histograms of the azimuth misfits (in degrees) of the compared parameters are shown in the insets of this and the subsequent figures.

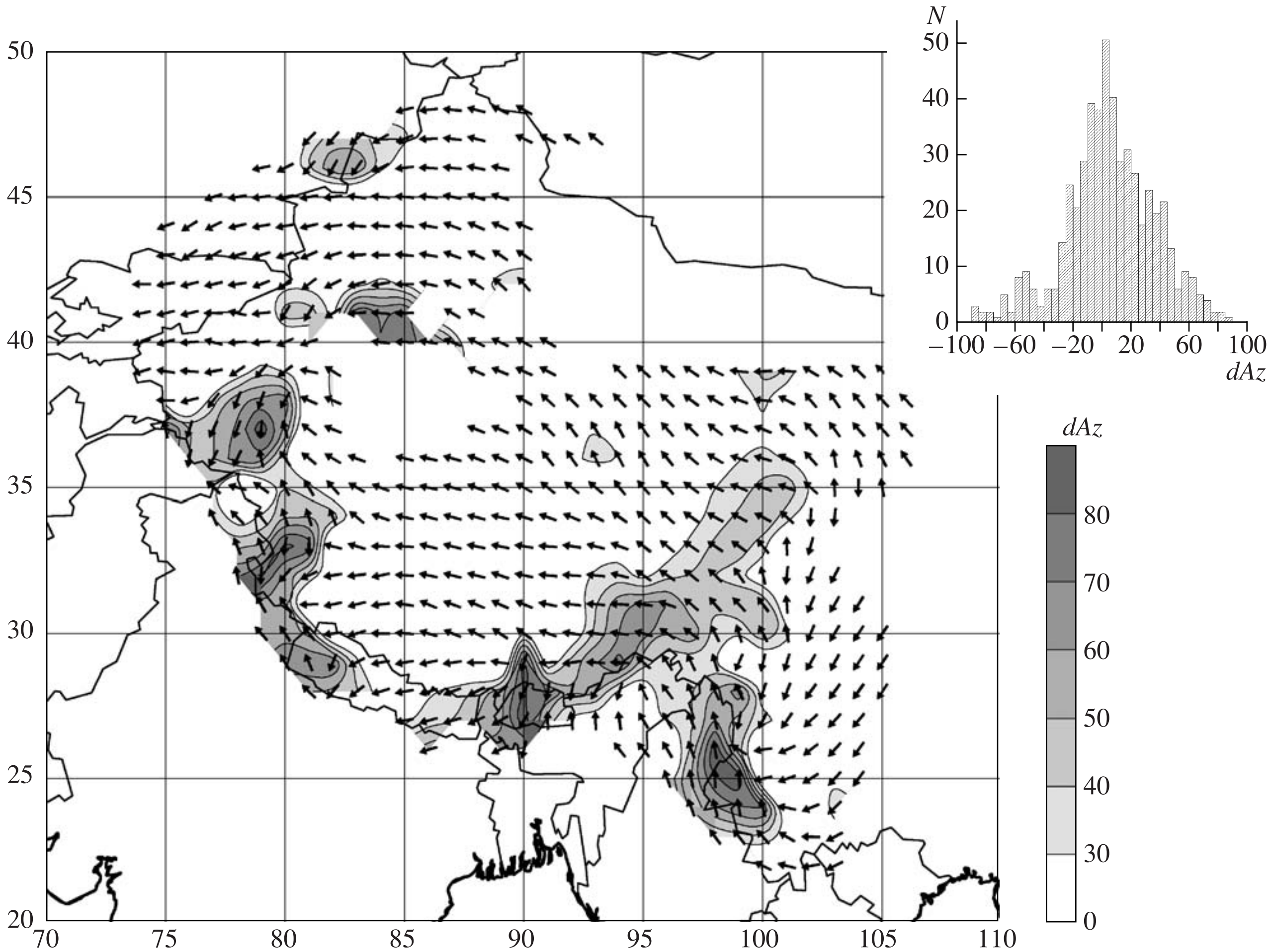

Fig. 6. Azimuth misfits of horizontal directions of seismotectonic strains over the period 1985–2004 and strains calculated from GPS data over the period 1998–2004 in a depth interval of $0 < H < 35$ km. Orientations of extension axes over the period 1998–2004 are shown by arrows.

the same directions. As seen from Fig. 6, maximum misfits of the stress and strain tensors are confined to regions of high spatial gradients of the strain axis directions, possibly related to the structural heterogeneity of these regions. On the other hand, maximum misfits in some areas of the region under study are due to the insufficient amount of the initial GPS data (Fig. 1) or the small number of earthquakes with a known focal mechanism. In this case, the discrepancies can be caused by errors of data interpolation. Large values of misfits can be confined to zones of deformations of the same type along both horizontal axes (compression or extension along all directions) or areas of small absolute values of recent horizontal movements. The elucidation of the origin of the disagreement is a goal of future research.

To gain insights into the variability of stress field parameters with depth, we compared the tensile axes obtained over the time interval 1985–2004 in depth intervals of $0 < H < 35$ km and $35 < H < 70$ km. The spatial distribution of tensile axes in the depth interval 35 km $< H <$ 70 km is presented in Fig. 7, where isolines show the azimuth misfit between the seismotectonic strain directions in the depth intervals $0 < H <$ 35 km and 35 km $< H <$ 70 km. As is evident from the inset in Fig. 7, the dispersion of the distribution of azimuth deviations increased. We associate the larger misfit between the directions of the seismotectonic strain axes with a depth-related change in the stress state. However, since the areal distribution of the initial information is nonuniform at depths greater than 35 km, the convergence of the principal stress axis directions within the study area is not quite good. As follows from the comparison results, a large part of the territory belongs to areas of a large misfit between the axis directions. Areas within which the stress axis directions remain invariable independently of the depth of initial data are also distinguished. The region studied contains areas of both stationary and depth-variable stress field which points to different deformation patterns in these areas. They can be due to the fact that the region contains blocks occurring at different depths and differing

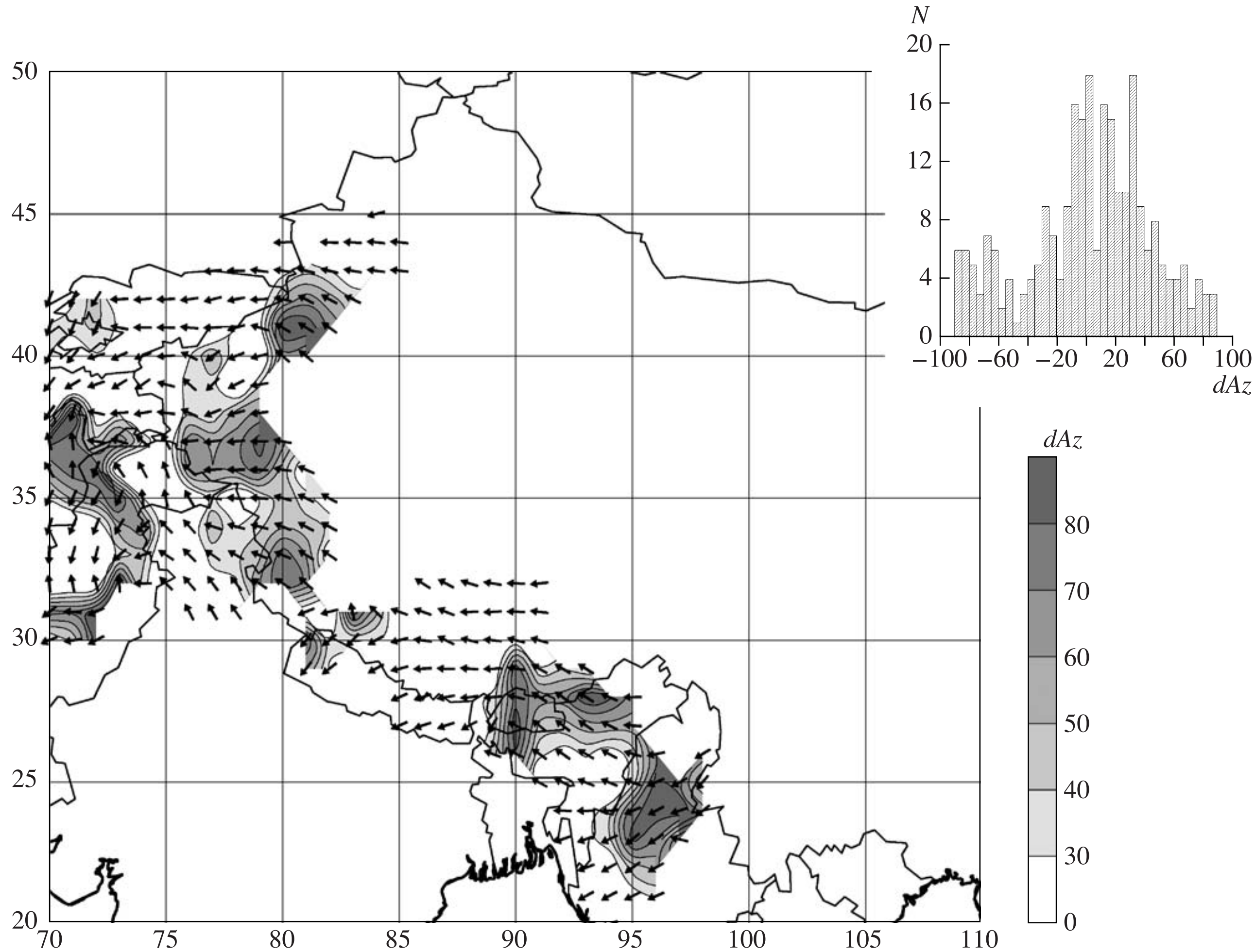

Fig. 7. Azimuth misfits between horizontal directions of seismotectonic strains in depths intervals of $0 < H < 35$ km and 35 km < $H < 70$ km over the period 1985–2004. Orientations of extension axes in a depth interval of 35 km < $H < 70$ km are shown by arrows.

in geological structure, which is confirmed by the spatial coincidence of anomalies in Figs. 6 and 7.

CONCLUSIONS

Reconstructions of the tectonic stress field in China from focal mechanisms of earthquakes over the periods of 1998–2004 and 1985–2004 in the depth interval $0 < H < 35$ km suggest that the stress field remains stationary with widening of the time interval under study. The comparison of the spatial distributions of seismotectonic tensile strain axes over the period of 1985–2004 and tensile strain rate tensor axes calculated from GPS data leads to the following conclusions.

(1) The seismotectonic strains and data of GPS measurements coincide in the larger part of the territory.

(2) The plastic strains in the near-surface part of the crust, which are not accounted for by the seismotectonic strain, are either small or have the same directions.

(3) Maximum misfits of the stress and strain tensors are confined to areas of high spatial gradients of the strain axis directions and are possibly related to the structural heterogeneity of the region.

(4) In some areas of the region, maximum misfits are due to an insufficient amount of the initial GPS data or a small number of earthquakes with known focal mechanisms. In this case, the discrepancies can be attributed to the errors of data interpolation.

(5) Large misfit values are confined to zones of deformations of the same type along both horizontal axes (compression or extension along all directions) or areas of small absolute values of recent horizontal movements.

The comparison of tensile axes obtained for the same time period in depth intervals of $0 < H < 35$ km and 35 km < $H < 70$ km leads to the following conclusions.

(a) Since the areal distribution of the initial information at depths greater than 35 km is nonuniform, the convergence of the directions of principal stress axes in the studied area could not be estimated in greater detail.

(b) As follows from the comparison results, a large part of the region belongs to areas of large misfits between axis directions.

(c) Areas are recognizable where the stress axis directions remain invariable independently of the depth of initial data.

ACKNOWLEDGMENTS

This work was carried out within the framework of the Russian–Chinese project "Sino-Russia Joint Researches on the Inner-Continent Seismo-Tectonics and New Techniques in Earthquake Observations and Prediction" and was supported by the Russian Foundation for Basic Research, project no. 06-05-64548a; by the Division of Earth Sciences, Russian Academy of Sciences (fundamental program no. 6 "Geodynamics and the Mechanism of Lithosphere Deformation"); and by the grants "Study on the New Methods for Possibility of Evaluation and Earthquake Prediction in China", no. 2004DFBA0005, and "China Scholarship Council Fund," no. 2004419001.

REFERENCES

1. Z. Chen, B. C. Burchfiel, Y. Liu, et al., "Global Positioning System Measurements from Eastern Tibet and Their Implications for India/Eurasia Intercontinental Deformation," J. Geophys. Res. **105**, 16 215–16 227 (2000).
2. Yu. G. Gatinskii, D. V. Rundquist, and Yu. S. Tyupkin, "Block Structures and Kinematics of Eastern and Central Asia from GPS Data," Geotektonika, No. 5, 3–19 (2005).
3. G. H. Gu, Y. Fu, and W. X. Wang, "Analysis on the Intensity of Horizontal Crustal Deformation in China Based on the Results of GPS Observations," Earthquakes **24** (2), 1–6 (2004).
4. O. I. Gushchenko, "Kinematic Analysis of Fracture Structures in a Reconstruction of Tectonic Stress Fields," in *Stress–Strain Fields in the Lithosphere,* Ed. by A. S. Grigor'ev and D. N. Osokina (Nauka, Moscow, 1979a), pp. 7–25 [in Russian].
5. O. I. Gushchenko, "Reconstruction of Megaregional Tectonic Stress Fields in Seismically Active Regions of Eurasia," in *Stress–Strain Fields in the Lithosphere*, Ed. by A. S. Grigor'ev and D. N. Osokina (Nauka, Moscow, 1979b), pp. 26–51 [in Russian].
6. O. I. Gushchenko, "Determination of Tectonic Stress Fields from Kinematic Analysis of Fracture Structures (in Relation to Seismic Hazard Prediction)," in *Nature of Tectonic Stresses in the Upper Crust and Methods of Their Determination* (Apatity, 1982), pp. 36–51 [in Russian].
7. O. I. Gushchenko, A. O. Mostryukov, and V. A. Petrov, "Structure of Recent Regional Stress Fields in Seismically Active Regions of the Crust of the Eastern Mediterranean Mobile Belt," Dokl. Akad. Nauk SSSR **312** (4), 830–835 (1990).
8. K. M. Larson, R. Burgman, R. Bilham, and J. T. Freymueller, "Kinematics of the India–Eurasia Collision Zone from GPS Measurements," J. Geophys. Res. **104** (B1), 1077–1093 (1999).
9. Z. S. Liang, Z. J. Ma, A. F. Niu, et al., "Approaches and Preliminary Results of Crust Movement Researches Based on the GPS in China," Earth Sci. Frontiers **10** (1), 71–79 (2003a).
10. Z. S. Liang, Z. J. Ma, X. Zhang, et al., "Horizontal Strain Field and Tectonic Deformation of China Mainland Related by Preliminary Result," Chinese J. Geophys. **46** (3), 352–358 (2003b).
11. Z. J. Ma, X. L. Chen, S. H. Ye, et al., "Study on the Recent Crust Movement Based on GPS in China," Sci. Sinica **46** (13), 1118–1120 (2001).
12. A. O. Mostryukov and V. A. Petrov, *Catalog of Focal Mechanisms of Earthquakes, 1964–1990* (WDCB, Moscow, 1994) [in Russian].
13. Sh. A. Mukhamediev, "Reconstruction of Tectonic Stresses from Strike-Slip Fault Motions: Mathematical and Physical Constraints," Dokl. Akad. Nauk SSSR **331** (4), 500–503 (1993).
14. Sh. A. Mukhamediev, T. P. Belousov, and A. N. Galybin, "Theoretical Modeling of Elastic Paleostress Fields from In Situ Indicators," Fiz. Zemli, No. 11, 47–61 (2005) [Izvestiya, Phys. Solid Earth **41** (11), 902–915 (2005).
15. Sh. A. Mukhamediev, A. V. Zubovich, and S. I. Kuzikov, "Identification of Crustal Blocks from GPS Data," Dokl. Akad. Nauk **40** (4), 539–542 (2006).
16. T. Parsons, "Tectonic Stressing in California Modeled from GPS Observations," J. Geophys. Res. **111** (2006).
17. V. A. Petrov, A. O. Mostryukov, and V. I. Lykov, "The Recent Field of Tectonic Stresses over the Territory of China," J. Earthquake Prediction Res. **3** (4) 509–527 (1994).
18. V. A. Petrov, A. O. Mostryukov, V. I. Lykov, and R. N. Petrova, "Structure of the Recent Tectonic Stress Field in the Crust of China and Adjacent Seismically Active Regions," in *Tectonophysics Today (in Honor of M.V. Gzovskii Jubilee)*, Ed. by V. N. Strakhov and Yu. G. Leonov (OIFZ RAN, Moscow, 2002), pp. 272–281 [in Russian].
19. Yu. L. Rebetsky, "Methods for the Reconstruction of Tectonic Stresses and Seismotectonic Strains Based on the Modern Theory of Plasticity," Dokl. Akad. Nauk **365** (3), 392–395 (1999).
20. Yu. L. Rebetsky, "A Review of Methods Used for the Reconstruction of Tectonic Stresses and Seismotectonic Strains," in *Tectonophysics Today (in Honor of M.V. Gzovskii Jubilee)*, Ed. by V. N. Strakhov and Yu. G. Leonov (OIFZ RAN, Moscow, 2002), pp. 227–243 [in Russian].
21. Yu. L. Rebetsky, *Tectonic Stresses and Strength of Natural Rock Masses* (IKTs Akademkniga, Moscow, 2007) [in Russian].
22. Yu. L. Rebetsky, A. V. Mikhailova, G. V. Rosanova, and E. V. Fursova, "II. Stress-Monitoring: The Modern Field of Regional Stresses in South-East Asia and Oceania. Principles of Quasiplastic Deforming of Fractured Media," J. Earthquake Prediction Res. **6** (1), 11–36 (1997).
23. S. F. Ying, L. R. Huang, L. Q. Guo, et al., "The Horizontal Deformation Observed by GPS in China," Seismol. Geol. **21** (4), 459–464 (1999).
24. A. V. Zubovich, R. T. Beisenbaev, Van Syaochan, et al., "Recent Kinematics of the Tarim–Tien Shan–Altai Region of Central Asia from GPS Measurements," Fiz. Zemli, No. 9, 31–40 (2004) [Izvestiya, Phys. Solid Earth **40** (9), 725–734 (2004)].